Science of the Total Environment 756 (2021) 143752

Contents lists available at ScienceDirect

Science of the Total Environment

journal homepage: www.elsevier.com/locate/scitotenv

Integrated air cathode microbial fuel cell-aerobic bioreactor set-up for enhanced bioelectrodegradation of azo dye Acid Blue 29

Mohammad Danish Khan [a,b], Da Li [b], Shamas Tabraiz [b], Burhan Shamurad [b], Keith Scott [b], Mohammad Zain Khan [a,*], Eileen Hao Yu [b,c,*]

[a] Industrial Chemistry Research Laboratory, Department of Chemistry, Aligarh Muslim University, Aligarh 202002, Uttar Pradesh, India
[b] School of Engineering, Newcastle University, Newcastle upon Tyne NE1 7RU, United Kingdom
[c] Department of Chemical Engineering, Loughborough University, Loughborough LE11 3TU, United Kingdom

HIGHLIGHTS

- More than 90% decolorization and 85% chemical oxygen demand removal achieved with integrated SMFC-aerobic bioreactor.
- Maximum cell potential achieved was 287.2 mV.
- *Proteobacteria* was shown 68.9% in anodic biofilm.
- *Acinetobacter* (17.1%) and *Pseudomonas* (12.1%) were most abundant at the bioanode and in the suspension, respectively.
- AB29 decolorization would contest with electrogenic bacteria for the electrons.

GRAPHICAL ABSTRACT

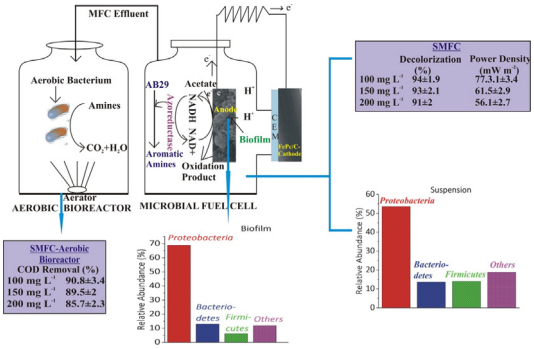

ARTICLE INFO

Article history:
Received 25 August 2020
Received in revised form 18 October 2020
Accepted 3 November 2020
Available online 26 November 2020

Editor: Defeng Xing

Keywords:
Acid Blue 29 degradation
Co-metabolism
Electrode biofilm
Integrated microbial fuel cell-aerobic bioreactor
Microbial community
Power generation

ABSTRACT

In this study, an azo dye (Acid Blue 29 or AB29) was efficiently degraded with acetate as co-substrate into less contaminated biodegraded products using an integrated single chamber microbial fuel cell (SMFC)-aerobic bioreactor set-up. The decolorization efficiencies were varied from 91 ± 2% to 94 ± 1.9% and more than 85% of chemical oxygen demand (COD) removal was achieved for all dye concentrations after different operating time. The highest coulombic efficiency (CE) and cell potential were 3.18 ± 0.45% and 287.2 mV, respectively, for SMFC treating 100 mg L^{-1} of AB29. Electrochemical impedance spectroscopy (EIS) revealed that the anode resistance was 0.3 Ω representing an entirely grown biofilm on the anode surface resulted in higher electron transfer rate. Gas chromatography coupled mass spectrometry (GC–MS) investigation demonstrated that initially biodegradation of AB29 started with the cleavage of the azo bond (-N=N-), resulted the biotransformation into aromatic amines. In successive aerobic treatment stage, these amines were biodegraded into lower molecular weight compounds. The 16S rRNA microbial community analysis indicated that at phylum level, both inoculum and dye acclimated cultures were mainly consisting of *Proteobacteria* which was 27.9, 53.6 and 68.9% in inoculum, suspension and anodic biofilm, respectively. At genus level, both suspension and biofilm contained decolorization as well as electrochemically active bacteria. The outcomes exhibited that the AB29 decolorization would contest with electrogenic bacteria for electrons.

* Corresponding author at: Industrial Chemistry Research Laboratory, Department of Chemistry, Aligarh Muslim University, Aligarh 202002, Uttar Pradesh, India.
E-mail address: E.Yu@lboro.ac.uk (E.H. Yu).

https://doi.org/10.1016/j.scitotenv.2020.143752

1. Introduction

More than 700,000 tons of synthetic dyes are manufactured around the world annually with over 100,000 dyes commercially available, of which the textile industries account for more than 50% and azo dyes are commonly used in these industries accounting for more than 70% of the global demand of industrial dyes (Berradi et al., 2019). The ecological issues created by textile industries have gained increased awareness for a very long time. Every year, out of total quantity of textile azo dyes produced, 10–15% is released through textile effluents around the world (Hassaan and Nemr, 2017). These dyes primarily emerge from coloring and finishing procedures and related with the water contamination and intended to oppose degradation with time, water, exposure to sunlight and soap. Wastewater releasing from textile industries has adverse effects in terms of color, total organic carbon (TOC), biological oxygen demand (BOD), pH (5–12), chemical oxygen demand (COD), recalcitrant organic compounds, salinity, ability to deplete dissolve oxygen, harmful effect on aquatic photosynthesis, human, flora and fauna (Solanki et al., 2013; Solís et al., 2012). Conventional wastewater treatment methods cannot treat azo dyes effortlessly because they are synthetically made and complex in structure (Wang et al., 2008). Till date, numerous physicochemical approaches have been established for the treatment of azo dyes containing wastewater, comprising advanced oxidation processes, such as ozonation oxidation, Fenton's reaction process, adsorption, coagulation/flocculation, catalytic degradation (Zou and Wang, 2017), however, high in operating cost and energy requirement and result in production of toxic pollutants due to breakdown of azo dyes (Hou et al., 2017). On the other hand, biological methods offer a low-cost and effective solution for the removal of color and organic matter simultaneously. However, using either aerobic or anaerobic biological processes only, complete degradation is difficult to achieve (Haug et al., 1991; Fernando et al., 2014).

Azo dyes consist of at least one azo groups (–N=N–) which is most alterable segments in the azo dye structure which can be reduced by accepting electrons from electron donors, however, produce carcinogenic and/or mutagenic compounds (Danish Khan et al., 2015). Biodecolorization through anaerobic reductive processes is typically very slow and requires an electron donor to establish the required reductive conditions (Khan et al., 2015; Solanki et al., 2013). Therefore, it is more beneficial to use microbial fuel cells (MFCs) in terms of reaction kinetics than traditional anaerobic bioreactors to achieve rapid reductive degradation of azo dyes (Sultana et al., 2015; Khan et al., 2014). In the recent years, MFC as a new technique has gained broad interests for directly treating dye containing wastewater and at the same time producing bioelectricity from organic co-substrates (electron donors) (Khan et al., 2017). A large number of co-substrates such as acetate, glucose, molasses, ethanol and other organic waste materials can provide reducing equivalents for the reduction process of azo dyes in MFCs (Pandey et al., 2016). Co-metabolism has been proven as the main removal mechanism for azo dye in the anode chamber of single chamber MFC (SMFC) under anaerobic condition. In other words, the simultaneous bioelectricity generation and reduction of azo dye are both driven by co-substrate oxidation and the two processes are competitive to each other as both reactions partially consume the electrons released from electrochemically active bacteria (EAB) after oxidation of co-substrate. In the anodic chamber of MFC, color can be greatly reduced as reductive azo bond cleavage occurs with the assistance of the azoreductase enzyme under anaerobic condition and biotransformation of azo dyeqs into their corresponding aromatic amines occurs (Oon et al., 2018; Wang et al., 2015). If the environment of anodic chamber is retained reductive after the azo dye biotransformation, the aromatic amine related compounds are hardly biodegraded further into lower molecular weight compounds and are observed to be resistant to this condition. However, aromatic amines are amenable to further degradation if the reductive environment is made oxidative under aerobic condition. Thus, the best methodology for accomplishing adequate biodegradation of azo dyes is to operate an integrated dual stage anaerobic–aerobic treatment process. Many researchers have shown this in past studies (Fernando et al., 2014; Thung et al., 2018). The use of SMFCs brings several benefits for the aim of pollutant removal. SMFCs generate higher power outputs and are easy to maintain compared to double chamber MFCs (DCMFCs) and therefore, could be considered more energy efficient (Khan et al., 2017). Utilizing sustainable and cost effective organic co-substrates, SMFCs can thus be the most appropriate technique for treating azo dyes containing wastewater. In addition, to resolve the harmful issues of aromatic amine formed after biotransformation of azo dyes in SMFCs, an aerobic post bio-treatment utilizing activated sludge systems is desirable. Compared to anaerobic digestion systems, MFCs can utilize oxygen having high redox potential as the final electron acceptor at the cathode (Logan et al., 2006) and oxygen reduction activity can be enhanced by using iron phthalocyanine (FePc) and palladium yttrium platinum core–shell–shell structure catalyst supported on carbon black (Burkitt et al., 2016; HaoYu et al., 2007; Liu et al., 2015; Yu et al., 2009). In earlier works, we revealed the efficient and swift treatment of Acid Navy Blue, Reactive Orange 16 utilizing SMFC-aerobic bioreactor set-ups in a sustainable way (Danish Khan et al., 2015; Sultana et al., 2015).

Acid Blue 29 (AB29) is a class of double azo anionic dye and generally utilized in textile, plastic, inks, paints, and leather factories. In this study, an SMFC with carbon brush anode and air cathode using low cost FePc/C oxygen reduction catalyst was employed. Different concentrations of azo dye AB29 laded wastewater along with the acetate as the co-substrate was supplied to the SMFC during the experiments. The work further included investigation of the electrochemical behavior of the SMFC system and pathway of biodegradation of AB29. The dye degrading, electron transfer bacterial communities and biofilm development were examined by using 16S rRNA sequencing and scanning electron microscope (SEM) analyses to observe change in behavior of bacteria in SMFC system.

2. Materials and methods

2.1. Chemicals and materials

A carbon brush was used as anode which was made up of carbon fibers wounded over two titanium wires twisted core constructed as detailed by Logan et al. (Logan et al., 2007). Gas diffusion layer (GDL) based carbon paper was procured from Quintech (H2315 I2 C6, Germany). Analytical grade chemicals were utilized in the study and purchased from Sigma Aldrich, United Kingdom.

2.2. Catalyst and electrode preparation

Carbon supported FePc (FePc/C) catalyst was prepared using the method described previously (HaoYu et al., 2007) using Vulcan XC-72 (Cabot) support. Briefly, carbon adsorbed with FePc was filtered and washed repeatedly with de-ionized water until the filtrate was pH > 5 and majority of H_2SO_4 removed and then dried at 110 °C for 12 h in an oven. Pyrolysis step was omitted. Nafion (10 wt%) (Aldrich) was used as the binder for preparing FePc/C catalyst ink which was coated on the GDL carbon paper for desired 1 mg cm^{-2} loading using paint brush. Carbon brush anode was rinsed in acetone (soaking 12 h) and then it was washed with distilled water and dried in an oven.

2.3. Reactor set-up, inoculation and operation

In the present study, the experimental SMFC set up was comprised of a glass compartment (300 mL) in which anaerobic condition was controlled (Fig. S1). Carbon brush (2 cm diameter x 5 cm length) was used as anode and FePc/C loaded carbon paper (25 cm^2) as air cathode and was positioned on the outside surface of the compartment. Cation exchange membrane (CEM, Fumasep FKB-PK-130, Fumatech, Germany)

was placed at the opening of 4 cm diameter made on the outer surface of compartment and was used to separate both the electrodes. The electrode spacing was 5 cm. Stainless steel mesh of size 25 cm^2 was placed along with cathode as current collector. A 1000 Ω external resistance was connected with titanium wire from both the ends which were connected with electrodes to complete the circuit. Effective working volume of SMFC was 250 mL in which dye wastewater and sludge ratio was 4:1. For further treatment of the effluent of SMFC, glass made aerobic bioreactor with working volume of 200 mL (150 mL SMFC effluent +50 mL acclimatized aerobic sludge) was operated to achieve complete degradation of intermediates formed during anaerobic degradation of AB29 in SMFC. The content of aerobic bioreactor was aerated by an air stone sparger using an aquarium pump to preserve the desired dissolve oxygen level. To acclimatize the systems before starting the experiment, the SMFC and aerobic bioreactor were inoculated with mixed-culture activated sludge collected from Tudhoe mills wastewater treatment plant, Durham, UK. During the acclimatization phase (start-up phase), the concentration of AB29 in 50 mM phosphate buffer was increased gradually from 10 mg L^{-1} to 100 mg L^{-1} and was fed into the SMFC along with activated sludge, acetate (1 g L^{-1}), mineral and vitamins (Fontmorin et al., 2018) and operated for more than 2 months. Prior to inoculation, the anodic medium was sparged with nitrogen gas for 15 min and the headspace of SMFC was also filled with nitrogen gas. When the electron donor (acetate) was almost exhausted and cell potential was dropped below 50 mV, replacement of the 80% anode content was carried out with fresh dye-containing medium, completing one operating cycle. Sludge in aerobic bioreactor was acclimatized with effluent generated in SMFC during the acclimatization phase. After acclimatization, in order to perform feasibility studies, three different concentrations of AB29 (100, 150 and 200 mg L^{-1}) along with acetate (1 g L^{-1}), mineral and vitamins were added to the SMFC. Decolorization process of AB29 under anaerobic condition using acclimated anaerobic sludge with open circuit was also carried out for comparison. The aerobic treatment to effluent of SMFC was provided for the duration of 24 h. The pH within SMFC remained 7.2–7.8 throughout the study. Experiments were performed in a dark and temperature-controlled box at 30 ± 1 °C. All experiments were carried out in duplicate.

2.4. Analysis of bioelectricity generation and AB29 degradation

The SMFC was operated over several fed-batch cycles to achieve the reproducible bioelectricity production with 1000 Ω external load during the acclimatization. A data logger (USB-6225 multifunction I/O device, National Instruments, US) was connected to the SMFC across the external resistance to monitor the voltage and current. The power density (PD, mW m^{-2}) was calculated using the Eq. (1)

$$PD = \frac{V^2}{RA} \tag{1}$$

where, V is cell potential (mV), R is external load (Ω) and A is area of the cathode (25 cm^2).

The coulombic efficiency (CE) is the ratio of actual coulombs of charge delivered to the anode to the total coulombs of charge generated provided that total COD is being transformed to biogenic electricity by taking the theoretical proportion of 4 mol of electrons/mol COD. The actual coulombs obtained were determined by integrating the current over time, therefore, the Eq. (2) was used to calculate the coulombic efficiency for SMFC operating in fed-batch mode measured over time t.

$$CE(\%) = \frac{M\int_0^t Idt}{V_{an}.b.F.\Delta COD} \tag{2}$$

where, M is molecular weight of oxygen, V_{an} is the volume of anode compartment, F is Faraday's constant and ΔCOD is the variation in COD during the experiment.

Samples collected during the experiment were first centrifuged (5000×, 30 min) and then filtered using PTFE membrane filters (0.22 μm) to separate suspended biomass. In order to confirm the overall treatment of AB29, samples were scanned in the full range (200–700 nm) in a UV–Visible spectrophotometer (JENWAY 7315, UK), whereas the variation in concentration of AB29 was determined by monitoring the variation in absorbance at 602 nm relating to –N=N– and then converting absorbance to concentration value using a calibration curve ($R^2 = 0.99$). The COD was monitored by using a HACH COD test kits and a spectrophotometer (DR6000, HACH Company, USA) to evaluate the organic removal efficiency.

The decolorization efficiency (DE) in SMFC and COD removal efficiency (RE) in integrated set-up were calculated using Eqs. (3) and (4)-

$$DE\ (\%) = \frac{(D_0 - D_t)}{D_0} * 100 \tag{3}$$

$$COD\ RE\ (\%) = \frac{(C_0 - C_t)}{C_0} * 100 \tag{4}$$

where D_0 is initial and D_t is the AB29 concentration at time t (hour) while C_0 is initial and C_t is the COD concentrations (mg L^{-1}) at time t (hour). The kinetics of AB29 decolorization was demonstrated by using first order kinetic model given in Eq. (5)-.

$$A = A_0\, e^{-kt} \tag{5}$$

where A and A_0 are the AB29 concentration (mg L^{-1}) at time t (hour) and initial concentration (mg L^{-1}), respectively, and 'k' is the rate constant.

2.5. Electrochemical characterization

Polarization curves (at closed circuit) were obtained at the stable state. Polarization data were measured by changing the external load from 20 to 2000 Ω using variable resistance box. Obtained data were utilized to calculate and draw power density curve. Electrochemical impedance spectroscopy (EIS) and cyclic voltammetry (CV) were performed during the last batch cycle of acclimatization period when SMFC was fed with 100 mg L^{-1} of AB29 along with acetate (1 g L^{-1}) and was stable and producing maximum cell potential. EIS and CV were performed by using an AutoLAb potentiostat (PGSTAT204, Metrohm, Netherlands). Two types of EIS measurements were performed, one for whole cell (SMFC) and the other for bioanode at the frequency range of 100 kHz to 10 mHz and 10 mV potential amplitude. EIS of whole cell (SMFC) was done in two-electrode configuration at open circuit voltage where working electrode was cathode and anode served as reference as well as counter electrode, whereas EIS of bioanode was done in three-electrode configuration at anode potential where bioanode, cathode and Ag/AgCl electrode were used as working, counter and reference electrodes, respectively. Reference electrode (Ag/AgCl) was placed near to the bioanode. In order to examine the electrochemical performance of SMFC for dye degradation, CV was performed over a range of −1 V to 1 V at the scan rate of 1 mV s^{-1}. The working and counter electrodes were anode and cathode of SMFC, respectively, and reference electrode was an Ag/AgCl electrode.

2.6. Scanning electron microscopy (SEM)

The bioanode surface was characterized using SEM (JEOL JSM-5600LV, JAPAN) to examine the bacterial attachment and the biofilm development at surface of anode at the end of the experiment. Prior to SEM analysis, fragments were cut from the anode and fixed overnight with 2% glutaraldehyde in Sorenson's phosphate buffer and then rinsed

twice in phosphate buffer solution of pH 7.2. The fragment samples were then dehydrated using 25, 50, 75 and 100% ethanol solutions. Fragment samples must be completely dry in order to get clear images. Therefore, samples were finally dried in a Baltec critical point dryer.

2.7. Gas chromatography-mass spectroscopy (GC–MS) analysis

An Agilent 7890B gas chromatograph (GC) coupled with an Agilent 5977B mass selective detector (MSD) was used to perform gas chromatography-mass Spectroscopy (GC–MS) analysis of the treated samples. An Agilent HP-5 fused silica capillary column (30 m × 0.25 mm I.D. X 0.25 μm film thickness) was used to accomplish chromatographic partition of the components. Extraction of the degraded samples (5 mL) was performed with ethyl acetate in proportion of 1:1 and then ethyl acetate was evaporated to dryness. Dried residue samples were finally dissolved in methanol (2 mL) for analysis. An Agilent 7683B autosampler was also used to inject prepared samples (1 μL). The following program was run: oven temperature of 60 °C (held for 5 min initially) to final temperature of 280 °C with a rise of 10 °C min^{-1} (held for 5 min finally). The temperatures of GC inlet and the GC/MSD interface were 280 and 310 °C, respectively. Helium as a carrier gas with a constant flow rate of 1 mL min^{-1} was used.

2.8. Microbial community analysis

The DNA of anodic biofilm and suspension was extracted by utilizing Fast DNA Spin Kit (MP Biomedicals, USA) as per the directions of manufacturer. The concentration and quality of the extracted DNA samples were analyzed by nanodrop (ThermoFisher, UK) and stored at −80 °C for further use.

Sequencing of DNA of microbial communities consisted of PCR amplification using primers 515F and 806R, targeting the V4 16S rRNA (Caporaso et al., 2011). The standard protocol consisted of a PCR performed with the GoTaq® Hot Start master mix (Thermo Fisher Scientific, UK) with the following conditions; initial denaturation (94 °C for 3 min), denaturation (94 °C for 45 s) for 35 cycles, annealing (50 °C for 30 s) and extension (70 °C for 90 s). Quality control (agarose gel check), library preparation comprising tagging, equimolar mixing and clean-up were finished. Sequencing of 16S rDNA amplicon was performed by using Illumina MiSeq V2 (2 × 250 bp).

Reads were pre-processed and denoised using QIIME 2 v2018.2.0 (https://qiime2.org) and DADA2 (Callahan et al., 2016) plugin, respectively. The obtained amplicon sequences variants (ASVs) were compared to the identical (99%) clustered MIDAS database v.2.0 (McIlroy et al., 2017) using a naive Bayes classifier trained on the amplified region. The relative abundance and non-metric multidimensional scaling (NMDS) graphs were made using microbiomeSeq, a package in R (Ssekagiri et al., 2017). Briefly, taxonomic assignments and associated ASV counts were imported and merged to a phyloseq object (McMurdie and Holmes, 2013). The ASV reads obtained were rarefied to ensure the same numbers of reads per sample (15,000) which were the fewest number in any sample. The phylogenetic trees were constructed using the procedure followed by Shamurad et al. (2019).

3. Results and discussion

3.1. Bioelectrical performance of SMFC

Acclimatization of bacteria in SMFC environment has significant role in color removal and can be enhanced by increasing the influent azo dye concentration step by step and by feeding co-substrate and azo dye simultaneously (Kong et al., 2018). In our study, the newly acclimatized bacteria and biofilm were adjusted to the electrogenic environment and gradually attached to the anode surface. During the course of study, the concentrations of AB29 were increased gradually to

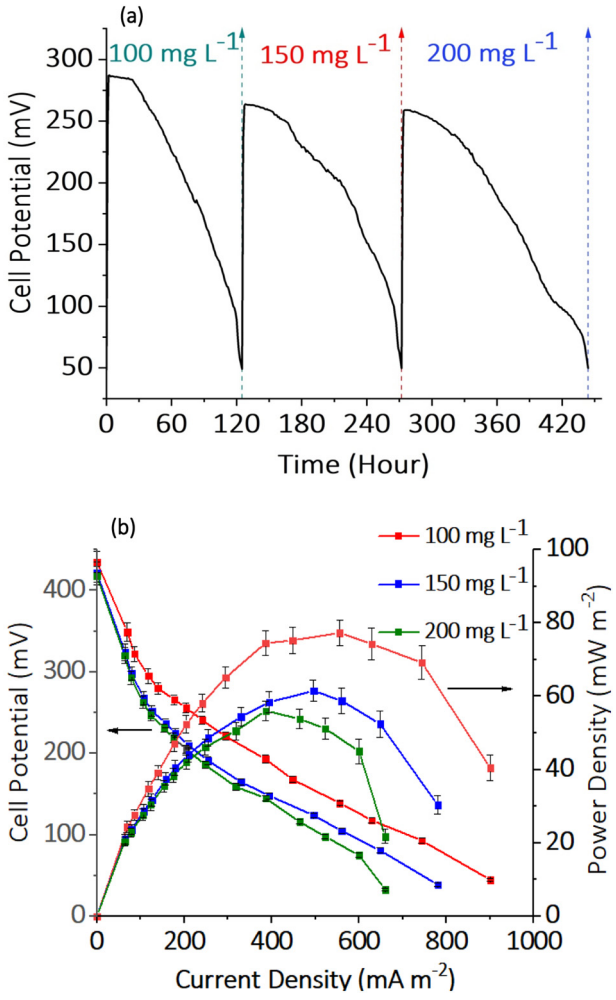

Fig. 1. (a) Effect of AB29 concentrations on bioelectricity generation (external load 1000 Ω) and (b) Polarization and power density curves of the SMFC with FePc/C modified cathode and the carbon brush anode containing AB29 and acetate (1 g L^{-1}) in 50 mM PBM.

200 mg L^{-1} (100, 150 and 200 mg L^{-1}). From Fig. 1a it is clear that, once acetate was started to consume by bacteria in the batch mode, peak of the cell potential started to decrease continuously and recovered after fresh addition of feed. The peak cell potential values were 287.2, 263.75 and 259.08 mV for 100, 150 and 200 mg L^{-1} azo dye, respectively, across an external resistance of 1000 Ω. The decent SMFC performance regarding bioelectricity production was observed because the acclimatized anaerobic sludge generally contains abundant electrogens. This agrees with 16S rRNA sequencing results presented in later part of the paper. The maximum cell potential was obtained for 100 mg L^{-1} of dye, however, the maximum cell potential decreased with further increase in AB29 concentration, which probably resulted from the increased inhibitory effect of AB29 against the activity of electricity producing bacteria (Sultana et al., 2015) or it may be ascribed to the fact that high concentration of AB29 needed more electrons to cleave azo bond. In a similar observation, Thung and co-workers reported a decrease in output voltage to 148.4 mV from 167.4 mV once Acid Orange 7 concentration was increased from 50 to 75 mg L^{-1} due to the reason that more electrons were transferred to azo dye rather than to the electrode after acetate oxidation (Thung et al., 2015). The output cell potential reached its least value at the end of the each cycle due to the co-substrate deficiency (Fig. 1a). Therefore, adequate quantity of biodegradable co-substrate is essential to be available to produce notable and continuous cell potential. Performance of the SMFC was evaluated by performing polarization and power density

curves and the obtained curves are presented in Fig. 1b. A maximum power density of 77.3 ± 3.4 mW m^{-2} was obtained in case of SMFC treating 100 mg L^{-1} AB29. However, maximum power densities were dropped to 61.5 ± 2.9 and 56.1 ± 2.7 mW m^{-2} for SMFC treating 150 mg L^{-1} and 200 mg L^{-1} AB29, respectively, possibly due to microbial inhibition with increase in dye concentration or higher concentration of dye required more electrons to break azo bond. In a similar work, Sun and co-workers reported treatment of Congo red (300 mg L^{-1}) in anode chamber of MFC with carbon paper electrodes (3 × 3 cm^2) using textile dyeing sludge and reported a maximum power density of 9 mW m^{-2} (Sun et al., 2016). Our results suggested that by using carbon brush anode which provided large surface area for bacterial attachment and FePc/C cathode for higher oxygen reduction activity, high power density in SMFC can be achieved.

3.2. Dye degradation in SMFC-aerobic bioreactor system

The UV–Vis spectra of the pure AB29 sample, SMFC treated effluent samples and the effluent samples after aerobic treatment were scanned in full range in spectrophotometer and are presented in Fig. 2a. The spectrum of pure AB29 displayed three different noticeable absorption peaks in the UV region represented benzene ring (232 nm) and naphthalene rings (309 and 389 nm) and one absorption peak in the visible region at 602 nm represented azo linkage (–N=N–) and accountable for the dark blue color of the AB29. The presence of absorption peaks in the anaerobically treated effluent exposed the existence of some biodegraded aromatic amine related products. However, the disappearance of any typical absorption peak in the aerobically treated effluent indicated that AB29 was fully biodegraded in an integrated SMFC– aerobic bioreactor treatment process.

In view of the characteristic absorption spectrum of the pure dye with a typical absorption band at λ_{max} = 602 nm due to azo bond, the DE (%) of the AB29 in the anolyte of the SMFC was calculated by monitoring the absorbance drop at 602 nm. Overall, the results showed that color was removed significantly due to reductive cleavage of azo bond in anaerobically maintained SMFC. The variation of AB29 decolorization in SMFC related to operating time is presented in Fig. 2b. The results of different concentrations of dye i.e. 100, 150 and 200 mg L^{-1} were compared for their DEs. Before the SMFC experiment, adsorption test on fresh carbon brush was also performed and was found to be negligible. More than 90% of color was removed for all concentrations. However, DEs were different with operating time. In the SMFC, the AB29 decolorization in 125, 147 and 172 h already reached 94 ± 1.9, 93 ± 2.1 and 91 ± 2%, whereas the open circuit controls had much lower AB29 decolorization efficiencies which were 54.1 ± 1.8, 51.3 ± 1.6 and 49.5 ± 1.4% for 100, 150 and 200 mg L^{-1} AB29. This also indicated that in the electrochemically active environment of an SMFC anode, the transfer of reducing equivalents to the azo moiety was more effective compared to open circuit controls. The open circuit controls are equivalent to an anaerobic reactor where, due to the absence of a functional anode, the microbes must resort to using alternate terminal electron acceptors. It was noticeable that degradation time was increased with increase in dye concentration due to bacterial inhibition. Earlier study has also reported that when the dye concentration increased, the higher biotoxicity inhibited the microbial activity and growth and resulted in a decrease in decolorization efficiencies (Long et al., 2019). Decolorization of AB29 followed first-order kinetics. Many researchers have also presented the similar behavior (Quan et al., 2018; Yang et al., 2016). The rate constants were 0.023 (R^2 = 0.99), 0.0159 (R^2 = 0.98) and 0.0136 h^{-1} (R^2 = 0.99) for 100, 150 and 200 mg L^{-1} concentrations of AB29 (Fig. 2c). The observed decline in decolorization level was probably because of the reduced bacterial resistant against AB29 which were accountable for decolorization and electron transfer, which limited acetate oxidation, electron transfer and consequently the decolorization efficiency. In line

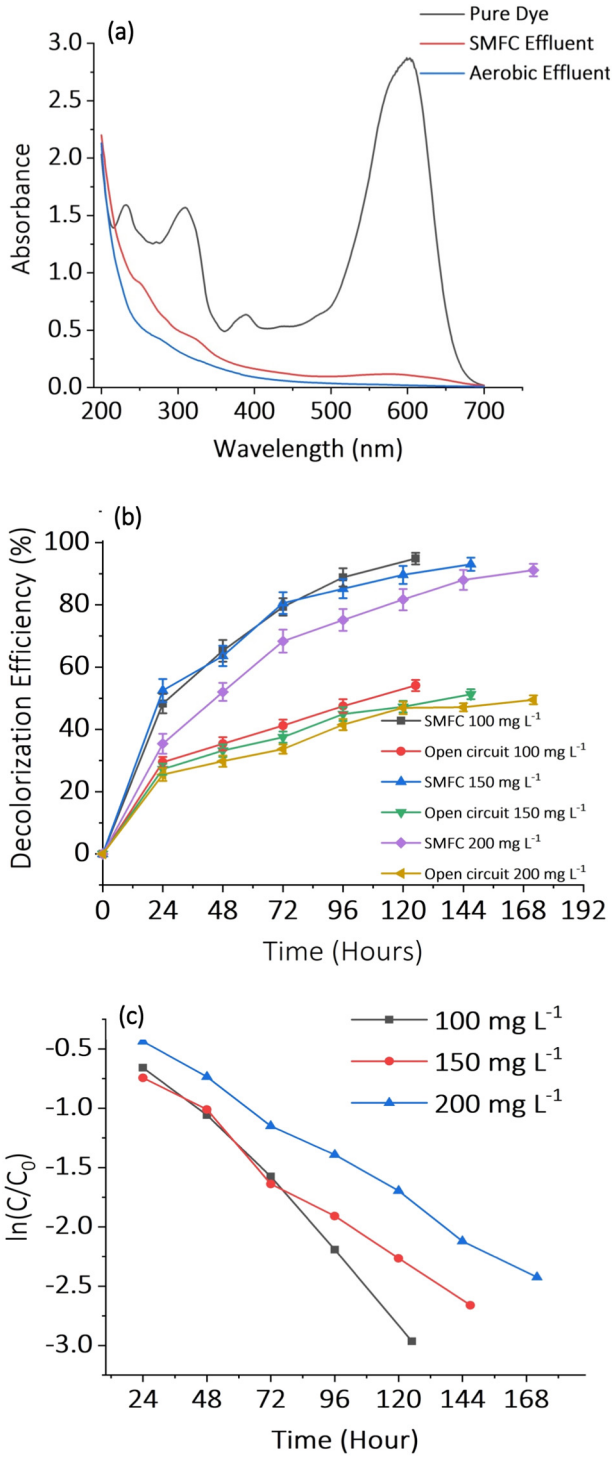

Fig. 2. (a) UV–visible absorption spectra for pure dye, SMFC effluent and aerobic effluent (b) Time course profile for decolorization of AB29 in SMFC and at open circuit and (c) Decolorization kinetics in SMFC.

with the outcome of current study, Fang et al. (2015) reported a high active brilliant red X-3B (ABRX3) concentration resulted in microbial inhibition and thus microbial population and activity decreased due to formation of toxic and recalcitrant products which could not be utilized by bacteria directly and due to this decolorization efficiency declined. Moreover, complete decolorization in SMFC does not mean complete mineralization due to biotransformation into aromatic amines although colorless but non-biodegradable under anaerobic condition. Therefore, to accomplish complete

degradation, SMFC treated effluents were transferred to aerobic bioreactor which was operated in batch mode.

3.3. Chemical oxygen demand removal and coulombic efficiency

The COD REs (%) in combined SMFC-aerobic bioreactor treatment process were calculated by monitoring the quantity of COD eliminated during the whole operation. The influent COD along with acetate (780 $mg_{COD}\ L^{-1}\ g^{-1}_{acetate}$) were 893, 950 and 1007 mg L^{-1} for 100, 150 and 200 mg L^{-1} AB29, respectively. The COD of influent samples increased with rise in AB29 concentration although the same quantity of acetate (1 g L^{-1}) was fed, this is due to the reason that AB29 itself contributed a certain quantity of COD to overall COD (100 mg L^{-1} of pure dye contains 113 mg L^{-1} of COD). The COD RE displayed enhancement during the experiment (Fig. 3a). The COD values were decreased sharply during initial 24 h, which could be attributed to the faster co-substrate usage during this period. COD REs in SMFC were 75.3 ± 2.8, 80 ± 2.9 and 74 ± 3.1% for 100, 150 and 200 mg L^{-1} AB29 fed SMFC after 125, 147 and 172 h of operation, respectively. It was also observed that operational time for COD removal was increased with increase in concentration of azo dye and it was highest for 200 mg L^{-1} fed SMFC. This could be brought about by the explanation that the COD removal extent could be confined by the higher concentration of AB29, as the dye toxicity might hinder bacterial actions in SMFC. In an MFC, respiration of EAB and anaerobic bacteria are the two biological activities lead to the removal of COD (Rózsenberszki et al., 2017). In this study, the reductive AB29 decolorization products were refractory aromatic amines, which were resistant to be treated by the anaerobes in SMFC and therefore the measured COD removal was primarily associated to the acetate consumption. Therefore, in order to accomplish adequate mineralization, effluent of SMFC was transferred to an aerobic bioreactor. After 24 h of aerobic post treatment, the final COD REs (%) were 90.8 ± 2.1, 89.5 ± 2 and 85.7 ± 2.3% for 100, 150 and 200 mg L^{-1} test concentrations, respectively (Fig. 3a).

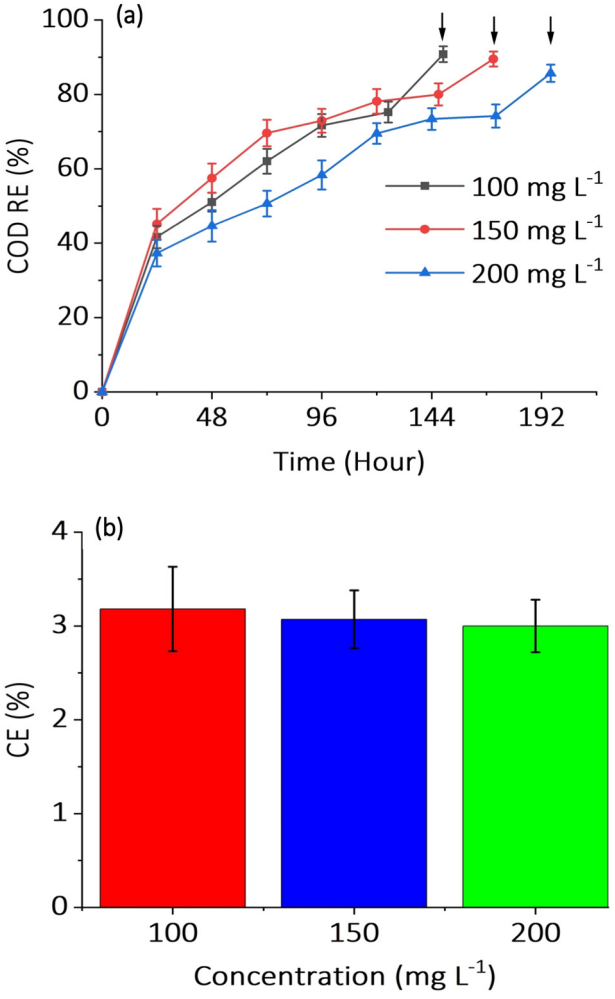

Fig. 3. (a) COD removal and (b) CEs in SMFC for three different azo dye concentrations (arrows displayed the COD removal after the successive aerobic treatment).

In most of the MFC studies, CE is widely monitored. In present study, CEs uncovered that most of the organic co-substrate consumed in SMFC was not utilized for bioelectricity production. The maximum CEs achieved in the SMFC were also dropped slightly with an increase in AB29 concentration; 100 mg L^{-1} (3.18 ± 0.45%) > 150 mg L^{-1} (3.07 ± 0.31%) > 200 mg L^{-1} (3 ± 0.28%), probably due to the increased electron consumption by increasing AB29 concentrations (Fig. 3b). It has been previously reported that azo dye competes with the bioanode for electrons (Sun et al., 2011). Other possible explanation for COD removal with low coulombic efficiency may be associated with the fact that additional factors such as consumption of electrons by microbes for growth, other electron acceptors (e.g., azo dye, O_2, SO_4^{2-}, CO_2) or competing methanogenesis and fermentation reactions could affect the CEs of bioelectrochemical systems (BESs) (Yang et al., 2018). The CEs acquired in this study were lower, however, relatively higher than the values (<1%) reported by other researchers, where they also presented decline in CEs due to the inoculation of MFC systems with mixed culture sludge. Also, a part of the electrons produced during oxidation of co-substrate were utilized for decolorization of azo dye, thus with increase in azo dye loading CE declined (Fang et al., 2015; Oon et al., 2018; Sultana et al., 2015).

3.4. Electrochemical studies

The CV is commonly used to study the electroactive species in the medium. Abiotic AB29 fed SMFC and the dye degradation products in anodic compartment were analyzed to monitor the presence of reduction end products using CV (Fig. 4a). The CV of pure AB29 dye formed redox couple at −0.20 V/−0.037 V vs Ag/AgCl. The degraded dye products in SMFC showed distinguishable oxidation peaks (forward scan) at −0.042 V and 0.25 V and the reduction peak (reverse scan) at −0.238 V, this could be the evidence of the biodegraded products contained in the SMFC. Thus, CV revealed that mechanism of AB29 decolorization in anode compartment is due to the breakdown of azo bond separating the benzene and naphthalene rings (Sun et al., 2016). The EIS works as a useful technique to reveal the bioelectrochemical phenomenon occurring in the BESs. This electrochemical technique has been extensively utilized to determine the internal resistance (R_{in}) of the BES. The internal resistance mostly is about solution resistance or ohmic resistance (R_s). This technique also tells activation (charge transfer) (R_{ct}) and Warburg (W) resistances, which are related to reaction kinetics (Sanchez-herrera et al., 2014; Sekar and Ramasamy, 2013). The complex (Z) results are shown in Nyquist plot (Fig. 4b). An equivalent circuit with the combination of R_s, R_{ct}, W and constant phase element (CPE) was made using results of EIS tests (Fig. 4b). Total internal resistance of the SMFC system was 45.5 Ω (R_s = 42.3 Ω and R_{ct} = 3.2 Ω). The reason for internal resistance of SMFC could be high spacing between the electrodes as well as the solution conductivity. Resistance ($R_s + R_{ct}$) for the bioanode was 0.3 Ω indicating fully grown biofilm on anode surface resulted in higher rate of electron transfer at the bioanode-electrolyte interface which may prompt higher biocatalytic activity of the anode and more electrons transfer to the cathode and hence enhanced bioelectricity generation.

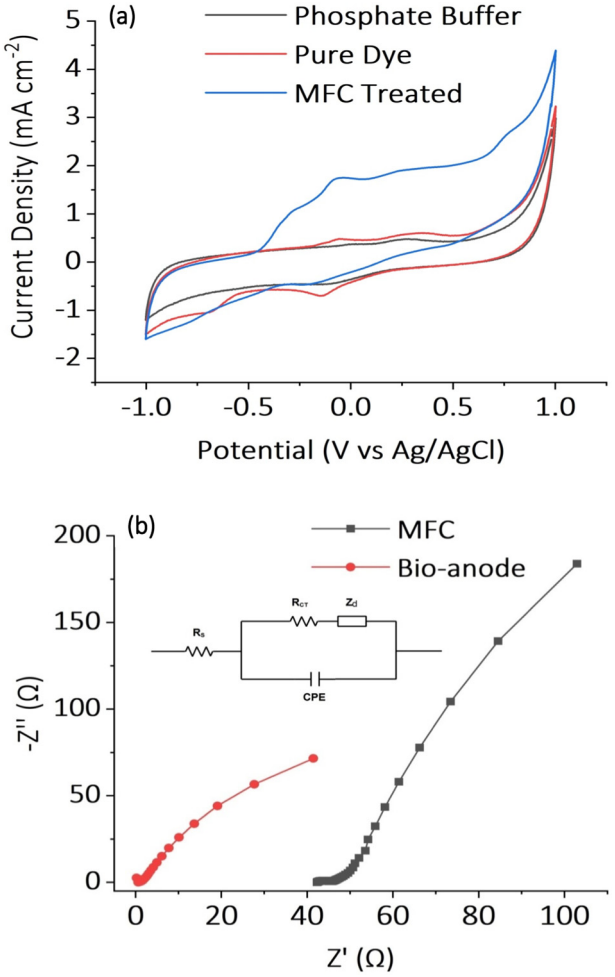

Fig. 4. (a) Cyclic voltammetry of pure dye (AB29) and SMFC treated effluent (100 mg L^{-1}) and (b) Nyquist plots of impedance spectra and circuit diagrams of the SMFC and bioanode treating azo dye.

3.5. Anodic biofilm characterization using scanning electron microscope

The EAB are denoted as anodophilic, electricigens and exoelectrogens. Biofilm on surface of anode was formed by the attachment and colonization of bacterial cells which worked as a biocatalyst that can biodegrade organic substrates and generate bioelectricity. The surface of carbon brush anode was imagined by SEM to visualize bacterial attachment and biofilm formation on the surface of anode. The bioanodes were taken out from the SMFC at the end of experiment. Fig. 5a showed the SEM images of bare carbon brush anode surface in the beginning of experiment. While, Fig. 5b and c showed the images for anode with a clear biofilm at the end of all experiments and exposed the existence of dense microbial community on the anode surface. Electron micrograph of bare carbon brush indicated an organized network of smooth and clearly visible carbon strands giving a large surface area for attachment of microbes. The sticky accumulation (biofilm) is mainly cocci and rod shaped, similar to what has previously been reported (Khan et al., 2020, 2018; Offei et al., 2016; Yang et al., 2012a). The biofilm formation on the electrode surface supported better transfer of electron; however, very dense biofilm limits electron transfer and thus reduce the output SMFC power. Microbial community analysis could give additional information about the importance of morphologies and their exact function.

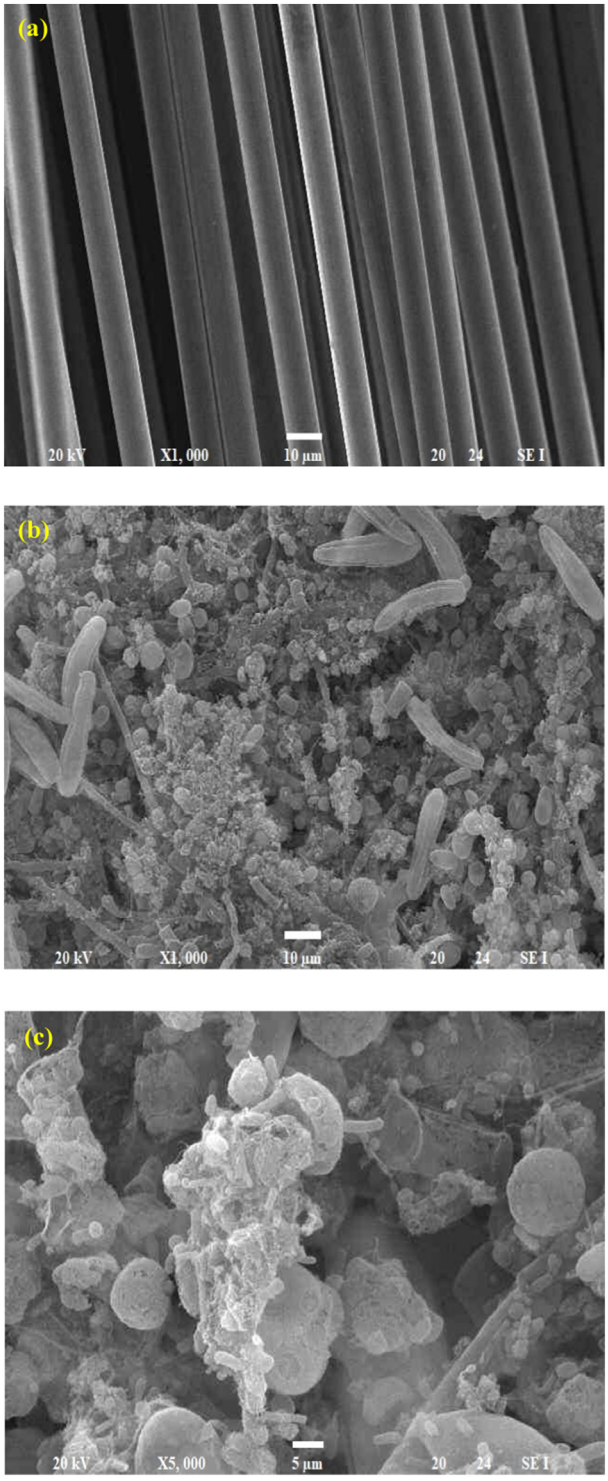

Fig. 5. SEM micrographs of the (a) Plain carbon brush (1000×) and (b,c) Anodic biofilm in the SMFC at magnifications of 1000× and 5000×.

3.6. Investigation of the AB29 degradation pathway via GC–MS

The intermediate compounds formed after the anaerobic treatment of AB29 in anode compartment of SMFC followed by aerobic treatment of SMFC effluent were investigated utilizing GC–MS technique. In order to examine the nature and the type of biodegraded products generated and to assure adequate mineralization of AB29, investigation of the degradation pathway is very crucial and presented in Fig. 6. Under

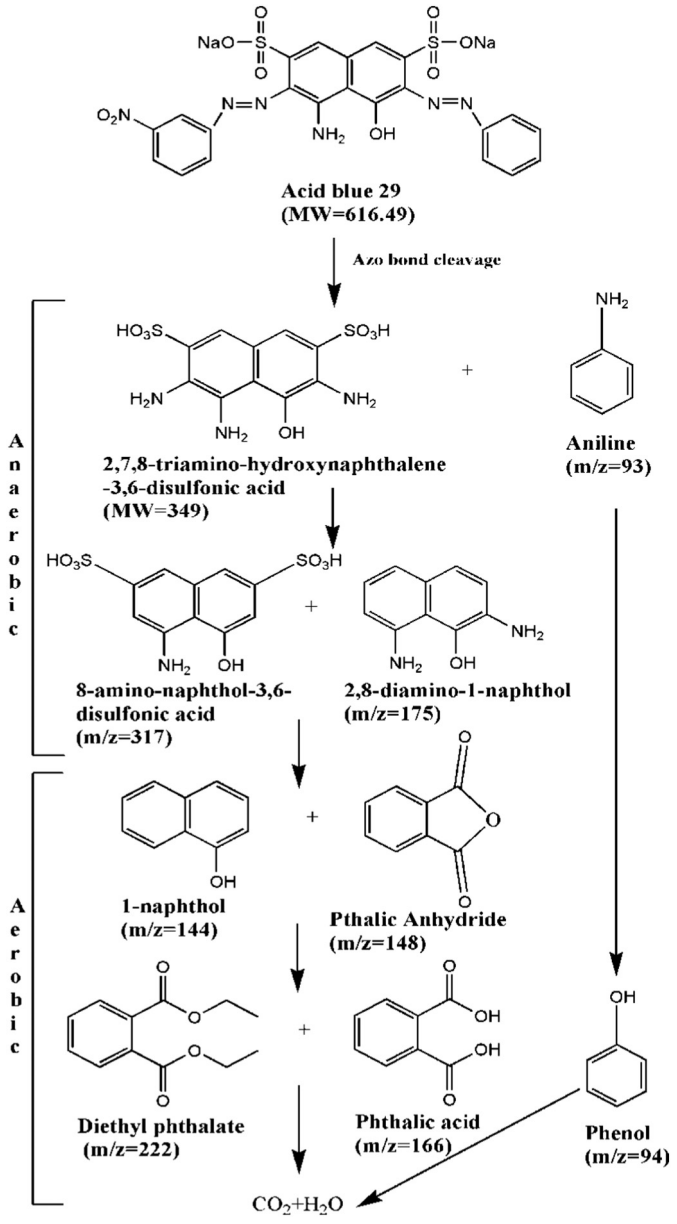

Fig. 6. Proposed degradation pathway of AB29 in integrated SMFC-aerobic bioreactor system.

anaerobic condition in MFC, reductive biotransformation of azo dye to aromatic amines occurs; however, the amines formed are hardly degraded further into simpler compounds under reductive condition and viewed as recalcitrant compounds. Amines are responsive to aerobes under aerobic condition and facilitate further degradation.

In this study, we proposed that initially reductive cleavage of azo bonds of AB29 resulted in the formation of 8-amino-naphthol-3,6-disulfonic acid ($m/z = 317$), 2,8-diamino-1-naphthol ($m/z = 175$) and aniline ($m/z = 93$). Moreover, an intermediate product 2,7,8-triamino-hydroxynaphthalene-3-6-disulfonic acid was also formed. In previous works, El Bouraie and El Din (2016) reported the formation of 2,7,8-triamino-hydroxynaphthalene-3-6-disulfonic acid after cleavage of azo bonds of Reactive Black 5 by *Aeromonas hydrophila* strain isolated from dye containing wastewater and Saratale et al. (2011) reported formation of 8-amino-naphthol-3,6-disulfonic acid after degradation Reactive Blue 172. The generation of the biodegraded products relies upon the bacterial diversity and the operating environment. The reductive breakdown of azo bonds (–N=N–) into aromatic amines was mainly due to the existence of azoreductase enzymes in anaerobic condition (Song et al., 2017), whereas the further oxidative degradation of aromatic amines was because of presence of several oxidoreductases in aerobic condition (Kalme et al., 2007; Qu et al., 2012). Furthermore, during electron withdrawal co-metabolic reaction may take place, co-substrates which functioned as electron donors, supported in the breaking of the azo bond and aromatic ring. The compounds of 8-amino-naphthol-3,6-disulfonic acid, 2,8-diamino-1-naphthol and aniline probably underwent deamination and desulfonation into 1-naphthol ($m/z = 144$), phthalic anhydride ($m/z = 148$) and phenol ($m/z = 94$) under aerobic condition. Thereafter it was further oxidized into diethyl phthalate ($m/z = 222$) and pthalic acid ($m/z = 166$). Similar observations were also reported in various earlier studies (El Bouraie and El Din, 2016; Saratale et al., 2011; Thung et al., 2018). These formed intermediates illustrated that the breakdown of aromatic ring occurred under aerobic condition. Lastly, these products could be further oxidized to carbon dioxide and water to achieve the complete treatment of AB29. In a similar work, Oon et al. (2018) reported that biodegradation of the azo dye New Coccine into aromatic amines occurred under anaerobic condition in MFC and further treatment of amines into simpler compounds under aerobic condition.

3.7. Microbial community of anodic biofilm and suspension

Microbial community analysis of acclimated sludge biomass of MFC is significant to understand the role of MFC regarding dye degradation and current production. To determine the overall performance of the MFCs, dye degrading, exoelectrogens, electricigens, fermentative and other types of microbes having definite roles can function collectively. The microbial community present in biofilm and suspension were analyzed by 16S rRNA gene sequencing and classified at phylum and genus levels.

Microbial community change in the suspension and anode biofilm in SMFC compared to inoculum at phylum and genus levels is shown in Fig. 7a and b. *Proteobacteria* (27.9%), *Plantomyces* (16.7%), *Chloroflexi* (16.1%), *Bacteroidetes* (11.8%), *Actinobacteria* (8.9%), *Verrucomicrobia* (6.9%) and *Fermicutes* (1.9%) were dominating phyla in the initial inoculum (Fig. 7a). After acclimatizing in dye wastewater containing co-substrate in SMFCs, the phyla *Proteobacteria*, *Firmicutes* and *Bacteroidetes* were the most abundant comprising 81.2 and 88.1% of the bacterial community in the suspension and biofilm, respectively, of the SMFC (Fig. 7a). *Proteobacteria* is a crucial community and has the ability to directly transfer electrons to the electrode and degrade a broad range of organic contaminants such as azo dyes (Forss et al., 2013; Ruiz et al., 2014). Fig. 7a presented relative abundance of *Proteobacteria* on bioanode (68.9%) and suspension (53.6%) which encouraged dye decolorization and bioelectricity generation in present study. *Bacteroidetes* are also described to be dominating phylum in systems degrading azo dyes in anaerobic conditions and potential exoelectrogens on the bioanode of MFCs (Quan et al., 2018). In current study, higher abundance of *Bacteroidetes* on bioanode (13%) and suspension (13.6%) were observed (Fig. 7a). *Firmicutes* are generally present in the MFCs and reported to be responsible for bioelectricity generation and effective dye decolorization (Fernando et al., 2013) which was present in higher abundance (14%) in suspension than bioanode (6.2%) in the current study (Fig. 7a). Various electrochemically active bacteria within these three phyla have been reported to be enriched in anode compartment of MFCs treating synthetic wastewater (Rathour et al., 2019). The most dominant genera from these three key phyla which include close relatives randomly selected from BLAST searches of the Genbank database are shown in the phylogenetic trees (Fig. 7c, d and e).

The relative abundance of the microbial community at the genus level in detail is shown in Fig. 7b. *Caldilinea* (11.9%), *Pseudomonas* (2.2%), *Flavobacterium* (2.9%) and *unassigned. Isosphaeraceae* (6.3%) were dominating species in the inoculum. The main enriched genera in the biofilm were; *Acinetobacter* (17.1%), *Xanthobacter* (10.8%), *Pseudomonas* (8.6%),

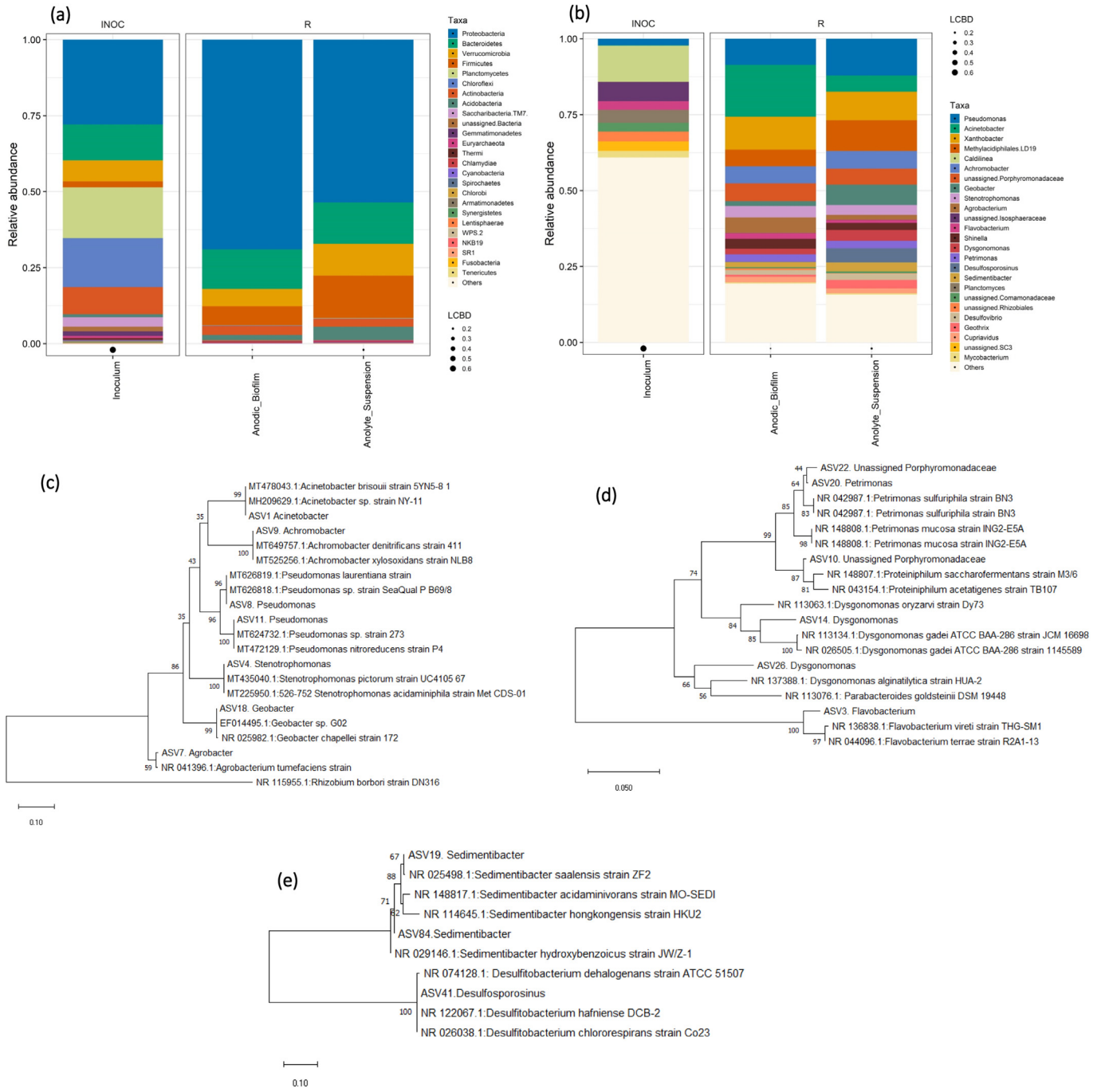

Fig. 7. Relative abundance of bacterial taxa at the (a) Phylum (b) Genus level and (c,d,e) Phylogenetic distance trees of key bacterial taxa in SMFC reactor and close relatives (c-*Proteobacteria*; d-*Bacteroidetes*; e-*Firmicutes*).

Achromobacter (5.6%), *Agrobacterium* (5.1%), *Stenotrophomonas* (3.8%), *Shinella* (3.3%), *Petrimonas* (2.5%), *Flavobacterium* (1.8%), *Dysgonomonas* (1.8%), *Sedimentibacter* (1.7%), *Geobacter* (1.6%) and *Desulfovibrio* (1.5%), whereas the dominant genera in suspension were; *Pseudomonas* (12.1%), *Xanthobacter* (9.4%), *Geobacter* (6.7%), *Achromobacter* (5.8%), *Acinetobacter* (5.4%), *Dysgonomonas* (3.5%), *Stenotrophomonas* (3.2%), *Sedimentibacter* (2.9%), *Shinella* (2.3%), *Desulfovibrio* (2.1%), *Petrimonas* (1.7%) and *Agrobacterium* (1.6%). From Fig. 7b, it is noticeable that *Acinetobacter* has high abundance on the bioanode and in the suspension of SMFC utilized acetate as a growth substrate and was helpful in transfer of electron and azo dye decolorization (Chen et al., 2010, 2018). *Geobacter* and *Pseudomonas* sp. produced biogenic electricity in the SMFC by excreting redox mediators that encouraged electron transfer to the anode extracellularly (Yang et al., 2012b). Furthermore, *Pseudomonas* was also capable of degrading dye and other aromatic compounds (Ge et al., 2015). *Achromobacter* is a fermentative bacteria, has been identified in SMFC and was capable of decolorizing azo dye in wastewater (Kong et al., 2018). *Desulfovibrio* reported in this work is also known as sulfate-reducing bacteria (SRB). In previous studies, the SRB have also been effectively utilized for the azo dye decolorization and biodegradation of intermediate compounds under anaerobic and sulfate-reducing environment (Miran et al., 2015). Moreover, *Stenotrophomonas*, *Petrimonas*, *Shinella*, *Desulfovibrio* and *Flavobacterium* cultivated in the SMFC were capable of electron transfer and degradation of dye (Dai et al., 2020).

Utilizing NMDS analysis, significant relationships were found among the community structure of anodic biofilm, suspension and the inoculum (Fig. S2). The structures of microbial communities sampled from anode biofilm and suspension of one SMFC were reasonably close to anode biofilm and suspension of other SMFC, respectively, since the two SMFCs were operated under the same conditions in duplicate. The inoculum community differed from biofilm and suspension community and formed in a separate direction, meaning that the bacterial community structure of inoculum at the start of experiment is highly differing to community at the end of experiment due to bacteria adaptation to SMFC environment. Such observed results indicated that the presence of an anode and azo dye provide supportive environment for the growth of exoelectrogenic and dye degradation bacteria together in the anodic compartment of the SMFCs, which is also reliable with previous works (Sun et al., 2013; Zhong et al., 2018).

4. Conclusions

In this work, an integrated SMFC-aerobic bioreactor was examined for azo dye degradation. Observed results noticeably build up the feasibility of treatment of dye laden wastewater and bioelectricity generation simultaneously. More than 90% of color removal was attained at different operating time for all dye concentrations. The SMFC-aerobic bioreactor combination was efficient for eliminating more than 85% of COD from dye containing wastewater for all concentrations. The maximum power density and CE were recorded as 77.3 ± 3.4 mW m^{-2} and 3.18 ± 0.45%, respectively, during the treatment of dye using carbon brush anode and FePc/C cathode. Efforts have been made to increase coulombic efficiencies and thus power generation in the SMFC system treating azo dye by utilizing immature activated sludge and iron phthalocyanine catalyst for better oxygen reduction activity at cathode which is more economical than using platinum catalyst. SEM results showed that bacteria were adhered on the anode surface developing a biofilm and subsequently, ability for power production was established by specific bacterial species. The GC–MS results showed that the initial bacterial attack on azo dye converted that into corresponding amines which were furthermore biodegraded to form low molecular weight end products. The 16S rRNA bacterial community analysis revealed that both dye degrading and electrogenic bacteria were considerably enriched in the SMFC system and were more dominating at bioanode. The interactions among microbial communities caused adequate AB29 decolorization and bioelectricity production in the SMFC and the culture acclimation was significant to accomplish effective dye degradation. The outcomes conclude that the AB29 can be successfully treated in combined two-stage process bringing about significant decrease in color and COD of the dye laden wastewater along with bioelectricity production using mixed culture sludge. However, it is important to monitor the influent dye concentration before treatment to obtain superior performance of SMFC.

CRediT authorship contribution statement

Mohammad Danish Khan: Conceptualization, Data curation, Methodology, Software, Investigation, Writing - original draft. **Da Li:** Formal analysis, Software. **Shamas Tabraiz:** Software, Formal analysis. **Burhan Shamurad:** Formal analysis. **Keith Scott:** Visualization, Resources. **Mohammad Zain Khan:** Supervision, Writing - review & editing, Project administration. **Eileen Hao Yu:** Supervision, Writing - review & editing, Project administration.

Declaration of competing interest

The authors declare that they have no known competing financial interests or personal relationships that could have appeared to influence the work reported in this paper.

Acknowledgements

This project was funded by EPSRC (EP/N009746/1), NERC (NE/L01422X/1) and Commonwealth Scholarship Commission (United Kingdom). Authors are also thankful to School of Engineering, Newcastle University, United Kingdom and Aligarh Muslim University, Aligarh for providing necessary research facilities. Data supporting this publication is openly available under an 'Open Data Commons Open Database License'. Additional metadata are available at: https://doi.org/10.25405/data.ncl.13200341.v1.

Appendix A. Supplementary data

Supplementary data to this article can be found online at https://doi.org/10.1016/j.scitotenv.2020.143752.

References

Berradi, M., Hsissou, R., Khudhair, M., Assouag, M., Cherkaoui, O., El Bachiri, A., El Harfi, A., 2019. Textile finishing dyes and their impact on aquatic environs. Heliyon 5. https://doi.org/10.1016/j.heliyon.2019.e02711.

Burkitt, R., Whiffen, T.R., Yu, E.H., 2016. Iron phthalocyanine and MnOx composite catalysts for microbial fuel cell applications. Appl. Catal. B Environ. 181, 279–288. https://doi.org/10.1016/j.apcatb.2015.07.010.

Callahan, B.J., McMurdie, P.J., Rosen, M.J., Han, A.W., Johnson, A.J.A., Holmes, S.P., 2016. DADA2: high-resolution sample inference from Illumina amplicon data. Nat. Methods 13, 581–583. https://doi.org/10.1038/nmeth.3869.

Caporaso, J.G., Lauber, C.L., Walters, W.A., Berg-Lyons, D., Lozupone, C.A., Turnbaugh, P.J., Fierer, N., Knight, R., 2011. Global patterns of 16S rRNA diversity at a depth of millions of sequences per sample. Proc. Natl. Acad. Sci. U. S. A. 108, 4516–4522. https://doi.org/10.1073/pnas.1000080107.

Chen, B.Y., Zhang, M.M., Ding, Y., Chang, C.T., 2010. Feasibility study of simultaneous bioelectricity generation and dye decolorization using naturally occurring decolorizers. J. Taiwan Inst. Chem. Eng. 41, 682–688. https://doi.org/10.1016/j.jtice.2010.02.005.

Chen, C., Tsai, T., Wu, P., Tsao, S., Huang, Y., 2018. Toxic/Hazardous Substances and Environmental Engineering Selection of Electrogenic Bacteria for Microbial Fuel Cell in Removing Victoria Blue R From Wastewater 4529. doi:https://doi.org/10.1080/10934529.2017.1377580.

Dai, Q., Zhang, S., Liu, H., Huang, J., Li, L., 2020. Sulfide-mediated azo dye degradation and microbial community analysis in a single-chamber air cathode microbial fuel cell. Bioelectrochemistry 131. https://doi.org/10.1016/j.bioelechem.2019.107349.

Danish Khan, M., Abdulateif, H., Ismail, I.M., Sabir, S., Zain Khan, M., 2015. Bioelectricity generation and bioremediation of an azo-dye in a microbial fuel cell coupled activated sludge process. PLoS One 10. https://doi.org/10.1371/journal.pone.0138448.

El Bouraie, M., El Din, W.S., 2016. Biodegradation of Reactive Black 5 by Aeromonas hydrophila strain isolated from dye-contaminated textile wastewater. Sustain. Environ. Res. 26, 209–216. https://doi.org/10.1016/j.serj.2016.04.014.

Fang, Z., Song, H.L., Cang, N., Li, X.N., 2015. Electricity production from Azo dye wastewater using a microbial fuel cell coupled constructed wetland operating under different operating conditions. Biosens. Bioelectron. 68, 135–141. https://doi.org/10.1016/j.bios.2014.12.047.

Fernando, E., Keshavarz, T., Kyazze, G., 2013. Simultaneous co-metabolic decolourisation of azo dye mixtures and bio-electricity generation under thermophillic (50°C) and saline conditions by an adapted anaerobic mixed culture in microbial fuel cells. Bioresour. Technol. 127, 1–8. https://doi.org/10.1016/j.biortech.2012.09.065.

Fernando, E., Keshavarz, T., Kyazze, G., 2014. Complete degradation of the azo dye Acid Orange-7 and bioelectricity generation in an integrated microbial fuel cell, aerobic two-stage bioreactor system in continuous flow mode at ambient temperature. Bioresour. Technol. 156, 155–162. https://doi.org/10.1016/j.biortech.2014.01.036.

Fontmorin, J.-M., Hou, J., Rasul, S., Yu, E., 2018. Stainless steel-based materials for energy generation and storage in bioelectrochemical systems applications. ECS Trans. 85, 1181–1192. https://doi.org/10.1149/08513.1181ecst.

Forss, J., Pinhassi, J., Lindh, M., Welander, U., 2013. Microbial diversity in a continuous system based on rice husks for biodegradation of the azo dyes Reactive Red 2 and Reactive Black 5. Bioresour. Technol. 130, 681–688. https://doi.org/10.1016/j.biortech.2012.12.097.

Ge, Y., Wei, B., Wang, S., Guo, Z., Xu, X., 2015. Optimization of Anthraquinone Dyes Decolorization Conditions with Response Surface Methodology by Aspergillus. vol. 53 pp. 327–332.

HaoYu, E., Cheng, S., Scott, K., Logan, B., 2007. Microbial fuel cell performance with non-Pt cathode catalysts. J. Power Sources 171, 275–281. https://doi.org/10.1016/j.jpowsour.2007.07.010.

Hassaan, M.A., Nemr, A. El, 2017. Health and environmental impacts of dyes: mini review. Am. J. Environ. Sci. Eng. 1, 64–67. https://doi.org/10.11648/j.ajese.20170103.11.

Haug, W., Schmidt, A., Nortemann, B., Hempel, D.C., Stolz, A., Knackmuss, H.J., 1991. Mineralization of the sulfonated azo dye Mordant Yellow 3 by a 6-aminonaphthalene-2-sulfonate-degrading bacterial consortium. Appl. Environ. Microbiol. 57, 3144–3149. https://doi.org/10.1055/s-2007-980050.

Hou, Y., Zhang, R., Yu, Z., Huang, L., Liu, Y., Zhou, Z., 2017. Accelerated azo dye degradation and concurrent hydrogen production in the single-chamber

photocatalytic microbial electrolysis cell. Bioresour. Technol. 224, 63–68. https://doi.org/10.1016/j.biortech.2016.10.069.
Kalme, S., Ghodake, G., Govindwar, S., 2007. Red HE7B degradation using desulfonation by Pseudomonas desmolyticum NCIM 2112. Int. Biodeterior. Biodegrad. 60, 327–333. https://doi.org/10.1016/j.ibiod.2007.05.006.
Khan, M.Z., Singh, S., Sreekrishnan, T.R., Ahammad, S.Z., 2014. Feasibility study on anaerobic biodegradation of azo dye reactive orange 16. RSC Adv. 4, 46851–46859. https://doi.org/10.1039/C4RA06716A.
Khan, M.Z., Singh, S., Sultana, S., Sreekrishnan, T.R., Ahammad, S.Z., 2015. Studies on the biodegradation of two different azo dyes in bioelectrochemical systems. New J. Chem. 39, 5597–5604. https://doi.org/10.1039/C5NJ00541H.
Khan, M.D., Khan, N., Sultana, S., Joshi, R., Ahmed, S., Yu, E., Scott, K., Ahmad, A., Khan, M.Z., 2017. Bioelectrochemical conversion of waste to energy using microbial fuel cell technology. Process Biochem. 57, 141–158. https://doi.org/10.1016/j.procbio.2017.04.001.
Khan, N., Khan, M.D., Nizami, A.S., Rehan, M., Shaida, A., Ahmad, A., Khan, M.Z., 2018. Energy generation through bioelectrochemical degradation of pentachlorophenol in microbial fuel cell. RSC Adv. 8, 20726–20736. https://doi.org/10.1039/c8ra01643g.
Khan, N., Anwer, A.H., Ahmad, A., Sabir, S., Sevda, S., Khan, M.Z., 2020. Investigation of CNT/PPy-modified carbon paper electrodes under anaerobic and aerobic conditions for phenol bioremediation in microbial fuel cells. ACS Omega 5, 471–480. https://doi.org/10.1021/acsomega.9b02981.
Kong, F., Ren, H.Y., Pavlostathis, S.G., Wang, A., Nan, J., Ren, N.Q., 2018. Enhanced azo dye decolorization and microbial community analysis in a stacked bioelectrochemical system. Chem. Eng. J. 354, 351–362. https://doi.org/10.1016/j.cej.2018.08.027.
Liu, X., Yu, E.H., Scott, K., 2015. Preparation and evaluation of a highly stable palladium yttrium platinum core–shell–shell structure catalyst for oxygen. Appl. Catal. B Environ. 162, 593–601. https://doi.org/10.1016/j.apcatb.2014.07.038.
Logan, B.E., Hamelers, B., Rozendal, R., Schröder, U., Keller, J., Freguia, S., Aelterman, P., Verstraete, W., Rabaey, K., 2006. Microbial fuel cells: methodology and technology. Environ. Sci. Technol. 40, 5181–5192. doi:https://doi.org/10.1021/es0605016.
Logan, B., Cheng, S., Watson, V., Estadt, G., 2007. Graphite fiber brush anodes for increased power production in air-cathode microbial fuel cells. Environ. Sci. Technol. 41, 3341–3346. https://doi.org/10.1021/es062644y.
Long, X., Cao, X., Liu, S., Nishimura, O., Li, X., 2019. The azo dye degradation and differences between the two anodes on the microbial community in a double-anode microbial fuel cell. Water Air Soil Pollut. 230. https://doi.org/10.1007/s11270-019-4325-4.
McIlroy, S.J., Kirkegaard, R.H., McIlroy, B., Nierychlo, M., Kristensen, J.M., Karst, S.M., Albertsen, M., Nielsen, P.H., 2017. MiDAS 2.0: an ecosystem-specific taxonomy and online database for the organisms of wastewater treatment systems expanded for anaerobic digester groups. Database 2017, 1–9. https://doi.org/10.1093/database/bax016.
McMurdie, P.J., Holmes, S., 2013. Phyloseq: an R package for reproducible interactive analysis and graphics of microbiome census data. PLoS One 8. https://doi.org/10.1371/journal.pone.0061217.
Miran, W., Nawaz, M., Kadam, A., Shin, S., Heo, J., Jang, J., Lee, D.S., 2015. Microbial community structure in a dual chamber microbial fuel cell fed with brewery waste for azo dye degradation and electricity generation. Environ. Sci. Pollut. Res. 22, 13477–13485. https://doi.org/10.1007/s11356-015-4582-8.
Offei, F., Thygesen, A., Mensah, M., Tabbicca, K., Fernando, D., Petrushina, I., Daniel, G., 2016. A viable electrode material for use in microbial fuel cells for tropical regions. Energies 9, 1–14. https://doi.org/10.3390/en9010035.
Oon, Y.S., Ong, S.A., Ho, L.N., Wong, Y.S., Oon, Y.L., Lehl, H.K., Thung, W.E., Nordin, N., 2018. Disclosing the synergistic mechanisms of azo dye degradation and bioelectricity generation in a microbial fuel cell. Chem. Eng. J. 344, 236–245. https://doi.org/10.1016/j.cej.2018.03.060.
Pandey, P., Shinde, V.N., Deopurkar, R.L., Kale, S.P., Patil, S.A., Pant, D., 2016. Recent advances in the use of different substrates in microbial fuel cells toward wastewater treatment and simultaneous energy recovery. Appl. Energy 168, 706–723. https://doi.org/10.1016/j.apenergy.2016.01.056.
Qu, Y., Cao, X., Ma, Q., Shi, S., Tan, L., Li, X., Zhou, H., Zhang, X., Zhou, J., 2012. Aerobic decolorization and degradation of Acid Red B by a newly isolated Pichia sp. TCL. J. Hazard. Mater. 223–224, 31–38. https://doi.org/10.1016/j.jhazmat.2012.04.034.
Quan, X., Xu, H., Sun, B., Xiao, Z., 2018. Anode modification with palladium nanoparticles enhanced Evans Blue removal and power generation in microbial fuel cells. Int. Biodeterior. Biodegrad. 132, 94–101. https://doi.org/10.1016/j.ibiod.2018.01.001.
Rathour, R., Patel, D., Shaikh, S., Desai, C., 2019. Eco-electrogenic treatment of dyestuff wastewater using constructed wetland-microbial fuel cell system with an evaluation of electrode-enriched microbial community structures. Bioresour. Technol. 285, 121349. https://doi.org/10.1016/j.biortech.2019.121349.
Rózsenberszki, T., Koók, L., Bakonyi, P., Nemestóthy, N., Logroño, W., Pérez, M., Urquizo, G., Recalde, C., Kurdi, R., Sarkady, A., 2017. Municipal waste liquor treatment via bioelectrochemical and fermentation ($H_2 + CH_4$) processes: assessment of various technological sequences. Chemosphere 171, 692–701. https://doi.org/10.1016/j.chemosphere.2016.12.114.
Ruiz, V., Ilhan, Z.E., Kang, D.W., Krajmalnik-Brown, R., Buitrón, G., 2014. The source of inoculum plays a defining role in the development of MEC microbial consortia fed with acetic and propionic acid mixtures. J. Biotechnol. 182–183, 11–18. https://doi.org/10.1016/j.jbiotec.2014.04.016.
Sanchez-herrera, D., Pacheco-catalan, D., Valdez-ojeda, R., Canto-canche, B., Dominguez-benetton, X., Domínguez-maldonado, J., Alzate-gaviria, L., 2014. Characterization of Anode and Anolyte Community Growth and the Impact of Impedance in a Microbial Fuel Cell. , pp. 1–10 https://doi.org/10.1186/s12896-014-0102-z.
Saratale, G.D., Saratale, R.G., Chang, J.S., Govindwar, S.P., 2011. Fixed-bed decolorization of Reactive Blue 172 by Proteus vulgaris NCIM-2027 immobilized on Luffa cylindrica sponge. Int. Biodeterior. Biodegrad. 65, 494–503. https://doi.org/10.1016/j.ibiod.2011.01.012.
Sekar, N., Ramasamy, R.P., 2013. Electrochemical Impedance Spectroscopy for Microbial Fuel Cell Microbial & Biochemical Technology Electrochemical Impedance Spectroscopy for Microbial Fuel Cell Characterization. https://doi.org/10.4172/1948-5948.S6-004.
Shamurad, B., Gray, N., Petropoulos, E., Tabraiz, S., Acharya, K., Quintela-Baluja, M., Sallis, P., 2019. Co-digestion of organic and mineral wastes for enhanced biogas production: reactor performance and evolution of microbial community and function. Waste Manag. 87, 313–325. https://doi.org/10.1016/j.wasman.2019.02.021.
Solanki, K., Subramanian, S., Basu, S., 2013. Microbial fuel cells for azo dye treatment with electricity generation: a review. Bioresour. Technol. 131, 564–571. https://doi.org/10.1016/j.biortech.2012.12.063.
Solís, M., Solís, A., Pérez, H.I., Manjarrez, N., Flores, M., 2012. Microbial decolouration of azo dyes: a review. Process Biochem. 47, 1723–1748. https://doi.org/10.1016/j.procbio.2012.08.014.
Song, L., Shao, Y., Ning, S., Tan, L., 2017. Performance of a newly isolated salt-tolerant yeast strain Pichia occidentalis G1 for degrading and detoxifying azo dyes. Bioresour. Technol. 233, 21–29. https://doi.org/10.1016/j.biortech.2017.02.065.
Ssekagiri, A., Sloan, T., Zeeshan, W., Ijaz, U., 2017. microbiomeSeq: An R package for analysis of microbial communities in an environmental context. ISCB Africa ASBCB Conf https://doi.org/10.13140/RG.2.2.17108.71047.
Sultana, S., Khan, M.D., Sabir, S., Gani, K.M., Oves, M., Khan, M.Z., 2015. Bio-electro degradation of azo-dye in a combined anaerobic–aerobic process along with energy recovery. New J. Chem. 39, 9461–9470. https://doi.org/10.1039/C5NJ01610J.
Sun, J., Hu, Y.Y., Hou, B., 2011. Electrochemical characteriztion of the bioanode during simultaneous azo dye decolorization and bioelectricity generation in an air-cathode single chambered microbial fuel cell. Electrochim. Acta 56, 6874–6879. https://doi.org/10.1016/j.electacta.2011.05.111.
Sun, J., Li, Y., Hu, Y., Hou, B., Zhang, Y., Li, S., 2013. Understanding the degradation of Congo red and bacterial diversity in an air-cathode microbial fuel cell being evaluated for simultaneous azo dye removal from wastewater and bioelectricity generation. Appl. Microbiol. Biotechnol. 97, 3711–3719. https://doi.org/10.1007/s00253-012-4180-3.
Sun, J., Cai, B., Zhang, Y., Peng, Y., Chang, K., Ning, X., Liu, G., Yao, K., Wang, Y., Yang, Z., Liu, J., 2016. Regulation of biocathode microbial fuel cell performance with respect to azo dye degradation and electricity generation via the selection of anodic inoculum. Int. J. Hydrog. Energy 41, 5141–5150. doi:https://doi.org/10.1016/j.ijhydene.2016.01.114.
Thung, W.E., Ong, S.A., Ho, L.N., Wong, Y.S., Ridwan, F., Oon, Y.L., Oon, Y.S., Lehl, H.K., 2015. A highly efficient single chambered up-flow membrane-less microbial fuel cell for treatment of azo dye Acid Orange 7-containing wastewater. Bioresour. Technol. 197, 284–288. https://doi.org/10.1016/j.biortech.2015.08.078.
Thung, W.E., Ong, S.A., Ho, L.N., Wong, Y.S., Ridwan, F., Lehl, H.K., Oon, Y.L., Oon, Y.S., 2018. Biodegradation of Acid Orange 7 in a combined anaerobic-aerobic up-flow membrane-less microbial fuel cell: mechanism of biodegradation and electron transfer. Chem. Eng. J. 336, 397–405. https://doi.org/10.1016/j.cej.2017.12.028.
Wang, L., Zhang, J., Wang, A., 2008. Removal of methylene blue from aqueous solution using chitosan-g-poly(acrylic acid)/montmorillonite superadsorbent nanocomposite. Colloids Surfaces A Physicochem. Eng. Asp. 322, 47–53. https://doi.org/10.1016/j.colsurfa.2008.02.019.
Wang, H., Luo, H., Fallgren, P.H., Jin, S., Ren, Z.J., 2015. Bioelectrochemical system platform for sustainable environmental remediation and energy generation. Biotechnol. Adv. 33, 317–334. https://doi.org/10.1016/j.biotechadv.2015.04.003.
Yang, S., Du, F., Liu, H., 2012a. Characterization of mixed-culture biofilms established in microbial fuel cells. Biomass Bioenergy 46, 531–537. https://doi.org/10.1016/j.biombioe.2012.07.007.
Yang, Y., Xu, M., Guo, J., Sun, G., 2012b. Bacterial extracellular electron transfer in bioelectrochemical systems. Process Biochem. 47, 1707–1714. https://doi.org/10.1016/j.procbio.2012.07.032.
Yang, H.Y., He, C.S., Li, L., Zhang, J., Shen, J.Y., Mu, Y., Yu, H.Q., 2016. Process and kinetics of azo dye decolourization in bioelectrochemical systems: effect of several key factors. Sci. Rep. 6, 1–9. https://doi.org/10.1038/srep27243.
Yang, Y., Luo, O., Kong, G., Wang, B., Li, X., Li, E., Li, J., Liu, F., Xu, M., 2018. Deciphering the anode-enhanced azo dye degradation in anaerobic baffled reactors integrating with microbial fuel cells. Front. Microbiol. 9, 1–10. https://doi.org/10.3389/fmicb.2018.02117.
Yu, E.H., Cheng, S., Logan, B.E., Scott, K., 2009. Electrochemical reduction of oxygen with iron phthalocyanine in neutral media. J. Appl. Electrochem. 39, 705–711. https://doi.org/10.1007/s10800-008-9712-2.
Zhong, D., Liu, Y., Liao, X., Zhong, N., Xu, Y., 2018. Facile preparation of binder-free NiO/MnO_2-carbon felt anode to enhance electricity generation and dye wastewater degradation performances of microbial fuel cell. Int. J. Hydrog. Energy 43, 23014–23026. https://doi.org/10.1016/j.ijhydene.2018.10.144.
Zou, H., Wang, Y., 2017. Azo dyes wastewater treatment and simultaneous electricity generation in a novel process of electrolysis cell combined with microbial fuel cell. Bioresour. Technol. 235, 167–175. https://doi.org/10.1016/j.biortech.2017.03.093.